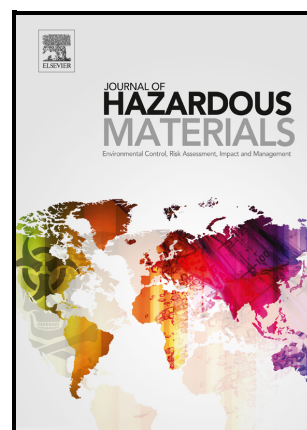# Journal Pre-proof

Discovery of a polyesterase from *Deinococcus maricopensis* and comparison to the benchmark LCC^{ICCG} suggests high potential for semi-crystalline post-consumer PET degradation

Konstantinos Makryniotis, Efstratios Nikolaivits, Christina Gkountela, Stamatina Vouyiouka, Evangelos Topakas

Please cite this article as: Konstantinos Makryniotis, Efstratios Nikolaivits, Christina Gkountela, Stamatina Vouyiouka and Evangelos Topakas, Discovery of a polyesterase from *Deinococcus maricopensis* and comparison to the benchmark LCC^{ICCG} suggests high potential for semi-crystalline post-consumer PET degradation, *Journal of Hazardous Materials,* (2023) doi:https://doi.org/10.1016/j.jhazmat.2023.131574

This is a PDF file of an article that has undergone enhancements after acceptance, such as the addition of a cover page and metadata, and formatting for readability, but it is not yet the definitive version of record. This version will undergo additional copyediting, typesetting and review before it is published in its final form, but we are providing this version to give early visibility of the article. Please note that, during the production process, errors may be discovered which could affect the content, and all legal disclaimers that apply to the journal pertain.

Discovery of a polyesterase from *Deinococcus maricopensis* and comparison to the benchmark LCC[ICCG] suggests high potential for semi-crystalline post-consumer PET degradation

Konstantinos Makryniotis[1], Efstratios Nikolaivits[1*], Christina Gkountela[2], Stamatina Vouyiouka[2], and Evangelos Topakas[1*]

[1]*Industrial Biotechnology & Biocatalysis Group, Biotechnology Laboratory, School of Chemical Engineering, National Technical University of Athens, Athens, Greece*

[2]*Laboratory of Polymer Technology, School of Chemical Engineering, National Technical University of Athens, Athens, Greece*

*Correspondence to: E. Topakas; vtopakas@chemeng.ntua.gr and E. Nikolaivits; snikolai@chemeng.ntua.gr

Abstract

Plastic pollution remains a significant environmental challenge, with conventional waste management strategies proving insufficient in addressing the problem. Enzymatic degradation has emerged as a promising alternative, with LCC[ICCG], an engineered metagenome-derived cutinase, being the most effective in degrading polyethylene terephthalate (PET), the most commonly produced and discarded polyester. However, more efficient PET-hydrolases are needed for the upscaling of a PET-waste biorefinery. In this regard, the study reports the characterization of a novel, phylogenetically distinct, thermophilic polyesterase from *Deinococcus maricopensis* (*Dm*PETase) and its comparison to LCC[ICCG]. *Dm*PETase is capable of degrading various synthetic polymers, including PET, polyurethane, as well as four semi-crystalline aliphatic polyesters. *Dm*PETase was found to be comparable to LCC[ICCG] at 50 °C in degrading semi-crystalline sections of post-consumer PET bottles, but it appeared to be less sensitive to crystallinity degree increase. This property makes *Dm*PETase a new template for protein engineering endeavors to create an efficient biocatalyst to be integrated into the bio-recycling process of PET waste, without the need for amorphization of the materials.

Environmental Implication

Polyethylene terephthalate (PET) is a widely used synthetic polymer, particularly hazardous as it accumulates in the environment, causing harm to both terrestrial and marine ecosystems. Enzymatic degradation has been shown to be an effective alternative to conventional waste management strategies, which have proven inadequate in tackling the plastic-waste problem. By identifying a thermophilic enzyme capable of degrading semi-crystalline materials and post-consumer PET bottles, without the need for amorphization, this work proposes a more energy-effective alternative for biocatalytic PET-waste reduction.

1. Introduction

Synthetic plastics are polymer materials that have become an indispensable part of contemporary life due to the multitude of applications they provide and the improved quality of life they offer. This has resulted in a sharp increase in global demand of plastics in the past decade, with approximately 400 million tons produced in 2021, predominantly destined for packaging and construction purposes [1]. Since the advent of widespread plastic production in 1950, roughly 60 % of used plastic has been discarded to the environment, being accumulated because of their high durability and resistance, creating a persistent problem [2–5]. As a result, plastic waste has become ubiquitous and can be found virtually everywhere, from the heights of mount Everest [6] to the depths of the Mariana Trench [7].

Recent studies have indicated that, globally, plastic waste primarily consists of polyesters, following the polyolefins [5]. PET was the most produced polyester resin in 2021 [1] with applications mainly in the manufacture of fibers for the clothing industry, and food and beverage containers, accounting for nearly 45 % of single-serve bottle production [8–10]. The majority of PET waste ends up in landfills, ultimately making its way into terrestrial and marine environments in the form of fragments and oligomers [11], causing harm to living organisms [12,13] and eventually entering the human food chain [14].

Conventional plastic waste management methods (landfills and incineration) seek to mitigate the growing volume of plastic waste, but they are limited by economic and environmental constraints. Eco-friendly options, such as recycling, present noticeable boundaries. For instance, despite the high collection rates of PET (up to 50 %), the quality of recycled PET final products tends to be lower than the virgin materials [15,16]. Biodegradable polymers have also been proposed as a green alternative, since they can degrade under environmental conditions. Their degradation is facilitated by the enzymatic machinery of various microorganisms breaking them down in oligo- and monomers [9,17]. Nonetheless, biodegradables have not been proven to be a panacea, as their natural degradation can take several decades, depending on environmental conditions [18–20]. To address this limitation, a more direct and controlled approach of degradation through enzymatic processes might accrue, leading to a bio-dependent, eco-friendly and feasible strategy for managing plastic waste.

In recent years, there has been a growing interest in discovering novel plastic-degrading enzymes, with a focus on polyesters, particularly PET, a major contributor to plastic pollution. The persistent nature of PET is attributed to the presence of aromatic components in its backbone, which hinder access by microorganisms and prevent biodegradation [21]. Most PET-degrading enzymes are bacterial and fungal carboxylesterases, belonging mostly to the cutinase family, which in nature conduce to the degradation of cutin, a natural waxy polyester [22]. Even though numerous enzymes have been discovered or engineered so far to efficiently degrade amorphous PET, degradation of the polymer's crystalline regions remains a challenge [23].

One of the central figures in amorphous PET biodegradation is the metagenome-derived LC-Cutinase (LCC), which has been extensively investigated for this ability. Recent advancements have led to the development of a thermostable variant of LCC (LCC[ICCG]) that exhibits high specificity towards PET and demonstrates remarkable efficiency in depolymerizing amorphized PET waste [24,25]. Concerning high crystallinity PET, it seems that LCC[ICCG] presents room for improvement while a latest study proved that further protein engineering might be the solution [26]. Notably, LCC[ICCG] is the only enzyme to be industrialized for PET biorecycling, with a processing temperature of 72 °C, and is expected to be implemented on a large scale in the near future [23,27].

Polymer biodegradation has been suggested to be more effective near the glass transition temperature (T_g), since chains are more accessible to enzymes, due to the abrupt conversion of the plastic state from glassy to rubbery [28,29]. For this reason, thermostability of PET hydrolases has been considered as an important feature, since T_g of PET is around 70 °C. However, the temporal aspect of PET degradation at those temperatures is very crucial, as studies demonstrated a correlation between polymer's crystallinity degree increase and reaction duration. Notably, PET storage at temperatures around its T_g for 48 h, initiates not only its "physical aging", but also the rearrangement of shorter polymer segments, leading to an increase in crystallinity, hindering the enzymatic depolymerization further [30,31]. Consequently, enzymatic degradation of amorphous PET at temperatures near its T_g, only makes sense for short reaction times, necessitating the utilization of enzymes with very high catalytic turnover, such as LCC[ICCG]. For lower reaction temperatures, polymer aging and crystallization are not an issue, hence slower enzymes can also be utilized.

In fact, amorphous PET degradation has been shown at milder temperatures of 30-50 °C by the benchmark mesophilic PETase from the bacterium *Ideonella sakaiensis* 201-F6 (*Is*PETase) [32] and its thermostable variants. The most recently-designed variant, FAST-PETase (a quintuple mutation of *Is*PETase), outperformed the thermotolerant LCC[ICCM], by presenting 5-fold higher degradation of amorphous postconsumer PET products at 50 °C [33]. This fact is indicating that protein engineering of non-thermophilic PET hydrolases could work as a greener route of PET degradation at lower temperatures.

In the present study, we report the discovery and biochemical characterization of a novel cutinase-like enzyme, designated as *Dm*PETase, from the bacterium *Deinococcus maricopensis*. *Dm*PETase's demonstrated polyesterase activity is compared to the benchmark PET-degrader LCC[ICCG] on a broad range of synthetic materials, including commercial plastics, such as PET and polyether polyurethane, as well as the biodegradable polybutylene succinate (PBS), polycaprolactone (PCL), polyhydroxy butyrate (PHB) and polylactic acid (PLA). Emphasizing on PET, our research focused on the effect of crystallinity on PET degradation, as PETases discovered to date have been shown to efficiently hydrolyze amorphous or low crystallinity PET, but their effectiveness is significantly limited at increased crystallinity [31]. To this aim, enzymatic reactions were conducted with virgin, amorphous and semi-crystalline powder, as well as with two types (transparent, colored) of post-consumer water bottles in their original and powdered form.

2. Materials and methods

2.1 Sequence and structural analysis of *Dm*PETase

The identification of the signal peptide for the full-length sequence of the E8U721 (UniProtKB) protein was performed using SignalP-6.0 [34]. A phylogenetic tree was constructed with MEGA 11.0 using the Neighbor-Joining method, which incorporated 25 sequences from the PDB database that were homologous to E8U721. The AlphaFold2 (AF2)-generated 3D structure of the enzyme was downloaded from the AlphaFold Protein Structure Database (UniProt ID: E8U721) and visualized by UCSF Chimera v1.15, excluding the native signal peptide (residues 1-33) and the residues 34-55, due to the absence of secondary structure information and their misalignment with

structures of other polyesterase structures. The electrostatic (Coulomb) potential surface was constructed and visualized by UCSF Chimera using the default parameters.

2.2 Cloning, heterologous expression and purification of *Dm*PETase and LCC[ICCG]

Genes encoding the cutinase-like enzyme from *D. maricopensis* (*Dm*PETase, UniProtKB ID: E8U721 excluding the native signal peptide) and quadruple variant of leaf branch compost cutinase (LCC[ICCG], variant F243I/D238C/S283C/Y127G, wild-type LCC UniprotKB ID: G9BY57 excluding the native signal peptide) were codon optimized for expression in *Escherichia coli* and synthesized in expression vectors pET22b(+) and pET26b(+), respectively, by GenScript Biotech B.V. (Netherlands). Chemically competent *E. coli* BL21(DE3) cells were transformed with each vector and grown for 16 h in Luria-Bertani (LB) plates supplemented with the proper selection antibiotic, ampicillin and kanamycin for *Dm*PETase and LCC[ICCG], respectively. The transformants were cultured in nutrient medium (LB or Terrific Broth) at 37 °C under agitation (180 rpm) and recombinant enzyme expression was induced by the addition of 0.2 mM isopropyl β-D-1-thiogalactopyranosidase (IPTG) for 16 h at 16 °C.

For purification of recombinant enzymes, *E. coli* cells were harvested by centrifugation at 4,000 x g for 15 min at 4 °C, resuspended in 50 mM Tris-HCl pH 8.0, 300 mM NaCl buffer and disrupted using an ultrasonic processor (VC 600, Sonics and Materials, Newtown, CT, USA) with four cycles of 60 s sonication (8 second pulses and 5 second pause, 50 % Duty Cycle), at 40 % amplitude. Clear lysates, collected after two rounds of centrifugation at 20,000 x g for 20 and 30 min, respectively, at 4 °C, were loaded onto immobilized metal-ion (Co^{2+}) affinity chromatography (IMAC) columns (Talon, Clontech; 1.0 cm i.d., 15 cm length) equilibrated with the same buffer. The columns were then washed with buffer and imidazole of varying concentration, 0-100 mM, as previously described [35]. The purity of the isolated *Dm*PETase and LCC[ICCG] was confirmed by sodium dodecyl sulphate-polyacrylamide gel electrophoresis (SDS-PAGE), using a 12.5 % polyacrylamide gel, and proteins concentration was calculated through conversion of the absorbance at 280 nm, via the molar extinction coefficient of the enzymes, determined by ProtParam tool from ExPASy [36]. The fractions containing the purified enzymes were dialyzed for 16 h at 4 °C against a 25 mM Tris-HCl pH 7.4, 150 mM NaCl, 20 mM imidazole buffer, for *Dm*PETase, and a 25 mM Tris-HCl pH 7.4, 150 mM NaCl buffer, for LCC[ICCG].

2.3 Biochemical characterization of recombinant DmPETase and LCC^{ICCG}

The cutinase activity of the enzymes was assayed using 1 mM p-nitrophenyl butyrate (pNPB) in 0.1 M phosphate-citrate buffer (pH 6.0), at 35 °C for 10 min, by adding 20 μL of enzyme preparation in 230 μL of substrate solution, and monitoring the release of p-nitrophenol (pNP) at 410 nm in a SpectraMax-250 microplate reader (Molecular Devices, Sunnyvale, CA, USA), equipped with SoftMaxPro software (version 1.1, Molecular Devices, Sunnyvale, CA, USA). Enzymatic activity is expressed in Units (U) as the amount of enzyme releasing 1 μmol of pNP per minute.

Kinetic studies on DmPETase and LCC^{ICCG} were performed with p-nitrophenyl water-soluble fatty acid esters with varying chain lengths, including p-nitrophenyl acetate (pNPA), pNPB, p-nitrophenyl octanoate (pNPO) and p-nitrophenyl decanoate (pNPD), which have two, four, eight and ten carbon atoms, respectively, under standard pNP assay conditions. Estimation of kinetic constants was accomplished through a non-linear regression model in GraphPad Prism 5 from GraphPad Software, Inc (USA).

The optimum temperature and pH of DmPETase and LCC^{ICCG} were determined by assaying enzyme activity on pNPB, under standard pNP assay conditions, in varying temperatures (30-90 °C) and pH values (5.0-9.0). Buffer systems used were 0.1 M citrate-phosphate (C-P, pH 5.0-6.0), 0.1 M sodium-phosphate (S-P, pH 6.0-8.0) and 0.1 M Tris-HCl (T-H, pH 8.0-9.0). The thermostability of DmPETase and LCC^{ICCG} was studied by measuring their residual activity, under standard pNP assay conditions, after incubation in 25 mM Tris-HCl pH 7.4, 150 mM NaCl buffer at temperatures ranging from 20-80 °C for up to 72 h. The effect of pH on the enzyme stability was studied by measuring enzymes residual activity, under standard pNP assay conditions, after their incubation in different buffer systems in the range of pH 5.0-10.0 for 24 h at 4 °C. Buffer systems used were 0.2 M citrate-phosphate (C-P, pH 3.0-6.0), 0.2 M sodium-phosphate (S-P, pH 6.0-8.0), 0.2 M Tris-HCl (T-H, pH 8.0-9.0) and 0.2 M glycine-NaOH (G-N, pH 9.0-10.0). Residual activity was then compared to the one of standard storage buffers, as described in paragraph 2.2.

2.4.1 Synthetic aliphatic polyesters, aliphatic-aromatic polyether and post-consumer PET

The initial form of target commercial synthetic aliphatic polyesters and aliphatic-aromatic polyether was pellets, except for amorphous PET film. Polyesters tested included aged PBS (initial grade NaturePlast PBE003, NaturePlast, France), PCL (CAPA 6500, Ravago Chemicals, Belgium), PET_I (PAPET clear, Lotte Chemical, UK), PET_{II} (destined for blow molding to commercial beverage bottle), PHB (Biomer P226, Biomer, Germany), PLA (4043D, NatureWorks, USA) and polyether PU (LPR7560, Coim, Laripur). The post-consumer PET used in this study was obtained from commercial, transparent and colored, water bottles.

2.4.2 Preparation and pretreatment of target polymers

To prepare the target polymers in powder form, pellets of PBS, PCL, PET_I, PET_{II}, PHB and PLA, amorphous PET film, as well as whole pieces of transparent and colored, post-consumer PET bottles (excluding caps and labels) were initially immersed in liquid nitrogen and subsequently milled in a PULVERISETTE 14 (FRITSCH Corp., Idar-Oberstein, Germany) at 17,000 rpm, supplementing liquid nitrogen in order to avoid sintering. Resulting powders (particle size < 500 um) of PBS, PCL, PET_I (cPET), PET_{II} (bPET), PHB, PLA and amorphous PET film (aPET) were dried under vacuum (300 mbar) under variable time and temperature conditions; PBS and PLA at 80 °C for 5 h, PCL at 40 °C for 24 h, aPET and cPET at 140 °C for 8 h, PHB at 60 °C for 2h and PU at 90 °C for 3h.

In order to investigate post-consumer PET degradation, pieces were hole-punched from various parts of the bottle, including the neck, shoulder, body and bottom (Figure S1 and S2). This sampling approach facilitated the examination of potential variations in PET degradation across different regions of the bottle. Resulting pieces from transparent bottle's shoulder (tsPET), body (tbdPET), and bottom (tbtPET), as well as colored bottle's shoulder (gsPET), body (gbdPET), and bottom (gbtPET) were all characterized by a diameter of 3.5 mm, while pieces from transparent and colored bottle's neck, tnPET and gnPET, respectively, had a diameter of 3.0 mm. For the

degradation of PET chips, it was assumed that enzymatic degradation occurs on the surface of the chips, with chips' thickness being considered negligible.

2.4.3 Properties of target polymers

The characterization of all materials (Table S1), including the determination of polymers' average molecular weight ($\overline{M_n}$), melting points of first and second heating cycle (T_{m1} and T_{m2}), relevant mass fraction crystallinity (x_c, %), crystallization point (T_c) and crystallization enthalpy (ΔH_c, J g^{-1}), was conducted in accordance with the methodologies outlined previously [37]. All samples were tested in duplicates.

2.5 Enzymatic hydrolysis of polymeric materials

2.5.1 Synthetic polyesters and polyether polyurethane materials

Enzymatic reactions were performed with 10 mg mL^{-1} of polymeric powder (PBS, PCL, PHB, PLA, PU) in 0.1 M sodium-phosphate buffer pH 7.0, at 50 °C, under agitation (1350 rpm) in an Eppendorf Thermomixer Comfort (Eppendorf, Germany) for 72 h. Reactions, of 0.5 mL, were initiated by the addition of 0.5 nmol of enzyme, while another 0.25 nmol were supplemented after 24 and 48 h. After 72 h (except for PCL reactions at 24 h) the residual material was isolated by centrifugation, triple washed with ultrapure water (Labaqua HPLC, ultrapure water system, Biosan, Latvia) and freeze-dried (Freeze dryer ALPHA 1-4, Braun Biotech International, Germany).

Biodegradation of synthetic polyesters was evaluated through mass loss and alteration of polymer's number average molecular weight ($\overline{M_n}$) and weight average ($\overline{M_w}$), determined by Gel permeation chromatography (GPC). GPC was performed using two PLgel MIXED-D 5 um columns (300 x 7.5 mm) (Agilent Technologies, Germany), in row, with mobile phase being 100 % tetrahydrofuran (THF >=99.9 % purity, Macron Fine Chemicals, Poland) for PCL, PLA and PU samples or chloroform (CHCl$_3$ >= 99.8 % purity, Fischer Chemical, U.K.) for PBS and PHB samples, at a flow rate of 1.0 mL min^{-1}. A refractive index detector (RID) (G7162A) at 650 nm, in an Agilent 1260 Infinity II LC instrument (Agilent Technologies, Germany) was utilized, calibrated with polystyrene standards of molecular weight from 162 to 500.000 g/mol (EasiVial PS-M 2 mL, Great Britain). Samples, 2 mg mL^{-1}, were prepared by dissolving the residual powders in THF or CHCl$_3$, using an Ultrasonic cleaner WUC-1,2 – 22 Litre

40 kHz (witeg Laboerthechnik GmbH, Germany) and filtered through 0.2 um syringe filters.

2.5.2 Virgin and post-consumer PET materials

Enzymatic reactions were conducted with 10 mg mL^{-1} of virgin and post-consumer PET powders (aPET, cPET, tPET, gPET and bPET) or post-consumer PET bottle pieces (tnPET, tsPET, tbdPET, tbtPET, gnPET, gsPET, gbdPET and gbtPET) in 0.1 M sodium-phosphate buffer pH 7.0, at 50 °C, under agitation (1350 rpm) in an Eppendorf Thermomixer Comfort (Eppendorf, Germany) for 72 h. Post-consumer PET samples were initially washed three times using ultrapure water solution with 1 % SDS and 20 % ethanol, subsequently triple washed with ultrapure water and finally freeze-dried. Reactions of 0.5 mL were initiated by the addition of 0.5 nmol of enzyme, while, in some cases, another 0.25 nmol were supplemented after 24 and 48 h, in order to investigate the importance of enzyme renewal in biodegradation performance as well as catalyst's stability. After 72 h the enzymatic reaction was terminated by adding HCl 6M at a final concentration of 0.1 % v/v, the supernatant was separated from the residual material with centrifugation and supplemented with 5 % v/v DMSO (Dimethyl sulfoxide, >= 99.9 % purity, Fischer Chemical, U.K.). PET powder was triple washed with ultrapure water (Labaqua HPLC, ultrapure water system, Biosan, Latvia) and freeze-dried.

Biodegradation of PET was evaluated through weight loss and quantification of the water-soluble hydrolysis products, determined by high performance liquid chromatography (HPLC). HPLC performed using a C-18 reverse-phase NUCLEOSIL®100-5 (Macherey-Nagel, Germany) with mobile phase 20 % v/v acetonitrile (>= 99.9 % purity, Fischer Chemical, U.K.), 20 % v/v 10 mM sulfuric acid (S.G. 1.84, >= 95 % purity, Fischer Chemical, U.K.) in 60 % v/v ultrapure water at a flow rate of 0.8 mL min^{-1}, using a photodiode array detector Varian ProStar at 241 nm, in an Agilent 1260 Infinity II LC instrument (Agilent Technologies, Germany). Quantification of PET degradation products was performed through calibration curves with standard concentrations in the range of 0.01–1 mM.

3. Results and discussion

3.1 Unique structural characteristics of the phylogenetically distinct *Dm*PETase

For expression and characterization, the UniProtKB sequence with ID E8U72, belonging to *D. maricopensis* LB-34 strain, was selected. The sequence was annotated as a triacylglycerol lipase and BLASTp against UniProtKB/SwissProt database revealed 60 % identity to PET hydrolases from *Thermobifida* species and LCC. This sequence has also been pointed out as a potential PET hydrolase by a previous study [38]. Phylogenetic analysis of characterized PET-degrading enzymes, with known 3D structure, using the Neighbor-Joining method, shows two distinct branches. One contains thermophilic enzymes and the other non-thermophilic enzymes belonging to Burkholderiales and marine *γ*-proteobacteria. In the thermophilic branch, the *D. maricopensis* enzyme forms its own distinct sub-branch, while the other contains enzymes from thermophilic actinomycetes and metagenomic or unidentified sources (Figure S3).

The overall structure of *Dm*PETase, as predicted by AF2, is nearly identical to other bacterial cutinases, with a root-mean-square deviation (rmsd) of 0.737 Å with LCC^{ICCG} (PDB ID: 7w1n) and 0.644 Å with *Is*PETase (PDB ID: 6eqh), as representative thermophilic and mesophilic PET-hydrolases (LCC^{ICCG} with *Is*PETase have a rmsd of 0.893 Å). The catalytic triad in *Dm*PETase is Ser185, His263 and Asp231, and the enzyme contains a single disulfide bond (DB) between cysteines Cys296-Cys312, which is common to the other two enzymes and one of the characteristics that distinguish PET hydrolases into two different classes (type I and type II) [23]. The wild-type LCC is a type I PET hydrolase, containing one BD, but LCC^{ICCG} has a second DB introduced through site-specific engineering at positions 238 (Asp238Cys) and 283 (Ser283Cys). *Is*PETase, on the other hand is a type II PET hydrolase, its second DB formed between Cys203 and Cys239 (Figure 1A).

When comparing the substrate-binding cleft of *Dm*PETase to the one from LCC^{ICCG} and *Is*PETase we see that all three enzymes are significantly similar. Figure 1A highlights the important residues for binding as indicated by the complex structure (PDB ID: 7VVE) of LCC^{ICCG} with 2-hydroxyethyl terephthalate (MHET) [39]. MHET binds to LCC^{ICCG} through residues Trp190, Val212, His242, Ile243, His164, Ala97,

Tyr95 and Met166, which are the same in *Dm*PETase (Trp210, Val233, His263, His184, Tyr117 and Met186) apart from two; Gly264 and Gly119. The position where Gly264 is in *Dm*PETase, there is Ile243 in LCC[ICCG], which is one of the mutated residues. The Ile243 substitution in LCC[ICCG] expands the substrate-binding tunnel and may increase the PET-binding capacity, while in the wild-type *Dm*PETase there is already a smaller residue at the same site. Comparing the width of the binding-site at that region (Figure 1B), we can see that for LCC[ICCG] and *Is*PETase it is 9.3 Å and 9.5 Å, respectively, while for *Dm*PETase it is 10.9 Å, which is significantly wider.

Previous research has demonstrated the impact of surface charges on the PET-degrading capability of various enzymes [40]. Sagong et al. proposed that negatively charged residues distal from the active site were more conducive to PET hydrolysis [41], while other studies suggested that an electrically neutral enzyme surface might reduce electrostatic repulsion with the polymer [42,43]. Figure S4 illustrates the distribution of electrostatic potential on the surface of *Dm*PETase next to that of LCC[ICCG] and *Is*PETase. It is evident that both LCC[ICCG] and *Is*PETase have positive charges on their front side, while *Dm*PETase is mostly neutral. Similarly, the bottom side of LCC[ICCG] and *Is*PETase is predominantly positively charged, while *Dm*PETase is mostly neutral with small areas of negative and positive charges. A clear distinction can also be observed on the top/back side of the enzymes, where *Dm*PETase has a region that is a considerably more negatively charged than the other two PET-hydrolases (green circles), whereas there is another small region at the top, near the active-site cleft (yellow circles), where *Dm*PETase is slightly less negatively charged than the other two enzymes. Interestingly, despite the fact that LCC[ICCG] and *Is*PETase are derived from entirely different sources and have very distinct properties, they display a remarkably similar electrostatic surface, which is dissimilar to the one of *Dm*PETase.

In a very recent study, a machine-learning tool in combination with evolutionary analysis was used to mutate LCC[ICCG], aiming in variants with increased activity on semi-crystalline PET. The most effective variant (LCCICCG_I6M) contained 6 point mutations, namely Asp53Thr, Ser67Lys, Ser133Arg, Thr188Pro, Glu208Gln, and Asn249Pro [26]. Surprisingly, all positions apart from one (Thr188Pro) are located on the surface of the enzyme and mostly involve mutation of uncharged residues into

positively charged or negatively charged residues into uncharged. At the respective positions *Dm*PETase contains either polar uncharged (Ser88, Gln229, Asn270) or charged residues (Arg74 and Asp155). Regardless, this work highlights the effect of surface residues on the ability of a PET hydrolase to degrade crystalline PET.

3.2 Biochemical characterization of *Dm*PETase and LCC[ICCG]

*Dm*PETase and LCC[ICCG] were recombinantly expressed, purified to homogeneity and concentrated in solutions, while their molecular weights (MW) were determined at 31 and 29 kDa, respectively, via their appearance as single bands on 12 % SDS-PAGE gel (Figure S5).

The optimal temperature for *Dm*PETase was determined to be 50 °C, while LCC[ICCG] showed its maximum activity at 60 °C. (Figure 2A). Both enzymes, especially LCC[ICCG], presented a thermostable profile retaining their activity at temperatures of 50 °C and 60 °C for *Dm*PETase (Figure 2C) and LCC[ICCG] (Figure 2D) respectively, after a 3-day incubation. Regarding pH effect, *Dm*PETase demonstrated maximum activity at pH 6.0, which comes in contrast to the conventional trend observed in most well-known PETases, mainly cutinases, which exhibit activity peak at neutral to slightly alkanine pH values [38,44], similar to LCC[ICCG] that displayed its highest activity at pH 8.5 (Figure 2B). Both enzymes' maximum stability was observed for T-H buffer system at pH 9.0 (Figure S6). The determination of kinetic constants for both *Dm*PETase and LCC[ICCG] (Table 1) on *p*NPA, *p*NPB, *p*NPO and *p*NPD indicated a typical Michaelis-Menten profile. The results demonstrated that both *Dm*PETase and LCC[ICCG] showed the highest catalytic efficiency towards *p*NPB followed by *p*NPA, *p*NPO and *p*NPD.

Summing up, *Dm*PETase's structure, protein sequence and biochemical characterization portray a thermophilic cutinase-like enzyme [45]. Further information and detailed commentary on biochemical characterization of both *Dm*PETase and LCC[ICCG] can be found in paragraph S1.1 of Supplementary Material.

3.3 Ability of *Dm*PETase and LCC[ICCG] to degrade polyester and polyurethane-based plastics

The capacity of *Dm*PETase and LCC[ICCG] to degrade synthetic polymers was tested for non- and bio-degradable synthetic plastics, including polyether PU and polyesters

such as PBS, PCL, PHB, PLA. Depolymerization degree of each plastic was assessed based on the percentage dry mass loss and changes in molecular weights ($\overline{M_n}$, $\overline{M_w}$), presented in Figure 3 and Table S3, respectively.

The results of the degradation study on PCL powder showed that LCC[ICCG] fully degraded (98.7 %) the material in just 24 h, while DmPETase led to a significant mass loss, degrading approximately 70 % of the material. The mass loss caused by DmPETase was also followed by molecular weight alterations in the remaining material, mainly in $\overline{M_n}$. The treatment of PBS powder with LCC[ICCG] and DmPETase led to a 79.6 % and 26.5 % mass loss, respectively, which in case of DmPETase was not accompanied by changes in the molecular weight of the residual material. The higher crystallinity of PBS (12 % higher than PCL, Table S2) may have made it more resistant to degradation in comparison to PCL, as its compact polymer structure would be tougher to break down. The degradation of PHB by both DmPETase and LCC[ICCG] resulted in a mass loss of approximately 15 % with no decrease in molecular weight. PHB has the highest initial weight average molecular weight among the tested polyesters, probably justifying its lower degradation yields in comparison to PBS and PCL. Moreover, the compact polymer backbone and presence of methyl side groups near the ester bonds might restrict enzyme accessibility. The enzymatic breakdown of PLA was very low as both polyesterases caused mass losses around 5 %. As with the aforementioned biodegradable polyesters, there was no molecular weight variation in the remaining powder. PLA's high molecular weight and T_g, as well as dense backbone, limit its susceptibility to degradation.

The degradation of the polyether PU powder was evidenced by a minor mass loss (2-5 %), as a result of the enzymatic action of DmPETase and LCC[ICCG]. Although the mass difference was negligible, the decrease in $\overline{M_n}$ by DmPETase was detectable at 8.2 %, implying a random cleavage mechanism resulting mainly in the release of insoluble products probably as a result of endo-manner action. Polyether PU, apart from the ether bonds, contains urethane bonds, however, (poly)esterases have been shown to be able to break this type of bonds too, highlighting their versatility [46,47].

In conclusion, both the novel DmPETase and the well-known PET degrader LCC[ICCG], exhibit significant polyesterase activity. To date, studies on LCC, have primarily focused on its PET-degrading ability rather than other polyester materials.

However, our study has demonstrated that LCC[ICCG] is more than just a PET hydrolase. Under the same temperature and enzyme concentration conditions, DmPETase demonstrated comparable performance. Despite the fact that all target polyesters exhibit diversity in their properties (Table S2) and consequently, it is challenging to ascertain which of these play a role in degradation of the material, a trend has emerged, wherein both cutinases exhibit a higher capacity for hydrolyzing polyesters with ester bonds spanning greater distance in their structure and monomers with non-substituted carbon atoms. Overall, both polyesterases exhibit similar selectivity for various polyesters and the combination of mass loss and molecular alterations might indicate a similar depolymerase mechanism for each polymer.

3.4 Comparison of DmPETase with LCC[ICCG] to degrade amorphous and semi-crystalline PET materials

Polymers' crystallinity degree is one of the main factors affecting enzymatic hydrolysis by restricting the enzymes' access to the hydrolyzable bonds [9]. Considering also that PET may exist as amorphous and semi-crystalline depending on its processing and thermal conditions [48], a wide range of three virgin (powders) and two post-consumer (chips and powders) PET grades with different mass fraction crystallinities were examined. Overall, across all tested PET samples, a range of crystallinity degrees, spanning from low (6 %) to high (40 %), was observed. All other thermal properties presented significant similarities, besides slightly decreased, T_{g1} of post-consumer PET grades compared to virgin grades, within rational bounds. A comprehensive discussion of the characterization of tested materials and additional analysis is present in paragraph S1.2 of Supplementary Material.

3.4.1 DmPETase degrades the crystalline part of postconsumer PET bottles at the same levels as LCC[ICCG]

This study aimed to evaluate the effectiveness of DmPETase and LCC[ICCG] polyesterases in degrading postconsumer PET bottles. Two types of water bottles, transparent and a green colored, were employed and divided into four different sections, with crystallinity degrees ranging from 10 % to 31 % (Table S1). The degradation of the chips by both enzymes was observed over a three-day period, monitoring the

generation of water-soluble products, the concentration of which is presented in Figures S10 and S11 for transparent and green bottle, respectively.

As expected, the neck was degraded more efficiently by both enzymes, compared to the rest of the compartments, as it was the one with the lowest crystallinity. LCC^{ICCG} was significantly more active than DmPETase on the neck of both bottle types, resulting in the release of approximately 30-fold more hydrolysis products after three days. Nevertheless, DmPETase exhibited comparable efficacy to LCC^{ICCG} in degrading the shoulder, body and bottom of both transparent and colored PET bottles, with no statistically significant differences in the release of hydrolysis products. Degradation of the crystalline parts of each bottle did not show statistically important differences, except for the degradation of the green bottom compartment by LCC^{ICCG}, which released 11-fold more products than the green shoulder. Interestingly, the degradation of shoulder and body compartments reveals a faster hydrolysis rate for LCC^{ICCG}, releasing more products in 1.5 days compared to DmPETase, which achieved the same level of degradation on the third day.

The degradation yields of transparent and colored bottles showed that parts of the green bottle were more susceptible to biodegradation. Specifically, the low crystallinity green bottle neck was 1.4- (from 12.6 to 17.2 $\mu g_{products}$/mm$^2_{chip}$) and 1.6-fold (from 0.44 to 0.71 $\mu g_{products}$/mm$^2_{chip}$) more degraded than the respective transparent compartment from LCC^{ICCG} and DmPETase, respectively. Apart from this, the green body part was hydrolyzed by DmPETase 6.4 times more (from 1 to 6 $ng_{products}$/mm$^2_{chip}$) than the transparent one.

However, the overall degradation yields were low even for the low crystallinity compartments, resulting in only 1-2 % degradation. Apart from crystallinity degree, the crystalline morphology can also be a significant factor in thermally crystallized PET, as it is the unstretched PET bottle neck crystallization temperature prior to blow-molding affects spherulites size and number. In samples of equivalent low crystallinity values, larger spherulites offer greater geometric impedance to mass transfer phenomena, something that is observed in PET oxygen permeability studies for $x_c <$ 20-30 % [49]. For the stretched and heat parts of the bottle (shoulder, body, bottom) strain-induced crystallization has happened during the stretch-blow molding, and the polymer chains are rearranged in parallel being closely packed affecting thus enzyme's

accessibility to the hydrolysable bonds. Furthermore, even though both enzymes degraded the crystalline parts of the bottles to the same extent, the yields did crystalline morphology of the bottles.

3.4.2 DmPETase activity is affected less by crystallinity increase compared to LCC[ICCG]

To investigate the effect of material morphology and crystallinity on enzyme activity, a subsequent investigation was performed by milling the bottles into powder and comparing with other PET materials of variable crystallinities, ranging from amorphous (7%) to semi-crystalline (41%), most of which are involved in bottle production. With milling, the different crystalline morphology of the stretched and unstretched bottle compartments obviously does not change, but the specific surface area for enzymatic degradation increases. The degree of depolymerization of each PET sample was assessed based on the amount of released water-soluble products released, as presented in Figure 4 and Table 2.

The results demonstrate that *Dm*PETase was able to degrade all tested PET samples, leading to the release of substantial amounts of water-soluble products. Table 2 shows that both *Dm*PETase and LCC[ICCG] exhibited the highest activity towards amorphous PET powder, producing a total of 119 μg/mgPET and 414 μg/mgPET water-soluble products, respectively. As the crystallinity of PET increased from 6 % (aPET) to 21 % (tPET and gPET), there was a 2.2- and 3.3-fold reduction in hydrolysis products by *Dm*PETase and a 2.5- and 4.2-fold reduction by LCC[ICCG], respectively. Notably, a further escalation of crystallinity to 40 % (cPET), resulted in a 15.3- and 22.6-fold decrease in PET degradation activity for *Dm*PETase and LCC[ICCG], respectively. Specifically, *Dm*PETase was able to degrade semi-crystalline PET, producing hydrolysis products at a concentration of 30.3 μg/mgPET, while LCC[ICCG] generated hydrolysis products at a concentration of 35.0 μg/mgPET. As anticipated, the progressive increase of PET crystallinity corresponded to a limitation of enzymatic degradation, as evidenced by the reduction in hydrolysis product concentration for both enzymes. It is worth noting that the correlation between the increase in PET crystallinity and the yield of degradation was exponential for both enzymes (Figure S12), but the decrease was sharper for LCC[ICCG]. Specifically, a significant 4-fold increase in crystallinity, from 6 % (aPET) to 21 % (tPET, gPET), led to a slight 2- to 4-fold decrease in enzymatic activity of both enzymes, while a further increase in crystallinity

to 40 %, caused a substantial reduction of dozens of times.

These findings are consistent with previous studies, which demonstrate that PET crystallinity levels up to 20 % may facilitate effective degradation, whereas higher values are associated with a significant reduction in enzymatic degradation yield [31]. Nevertheless, the depolymerization results of bPET, with a x_c of 36 %, contradict this trend, as despite its similar crystallinity to cPET (x_c of 40 %), its degradation capacity dropped by 2- and 4-fold by *Dm*PETase and LCC[ICCG], respectively. This outcome could be attributed to various material properties, such as the increased hygroscopicity and moisture absorption of cPET (according to the material datasheet), which potentially facilitated the diffusion of the enzymatic solution through cPET powder particles during the reaction, leading to more efficient degradation.

Emphasizing on post-consumer bottles, both *Dm*PETase and LCC[ICCG] demonstrated efficient degradation with 3-5 % and 10-15 % degradation yields, respectively, indicating that milling of the bottles, even without quenching, significantly enhances enzymatic degradation performance, due to the increase of the available surface area. Grinding of transparent and green bottle enhanced degradation by *Dm*PETase by 93- and 35-fold respectively, while LCC[ICCG] breakdown action was increased by 10- and 5-fold respectively, comparing to the sum of the hole-punched samples from various bottle compartments. In contrast to the bottle pieces case study, where the green bottle appeared more susceptible to biodegradation, the results from the powder hydrolysis suggested that the transparent bottle was degraded about 1.5-fold more, compared to green bottle powder, by both enzymes. It is possible that colorants, wax dispersants, and copolymer additives, which are perceptible in colored PET [50], might be released with grinding, possibly impeding enzymatic action.

Focusing more on the enzymatic perspective, Figure 5 highlights that the degrading activity of *Dm*PETase on amorphous PET is approximately 3.5-fold lower than that of LCC[ICCG]. However, LCC[ICCG] displays 3.0 and 2.5 times more efficient enzymatic degradation of transparent and green PET bottle powders, respectively. LCC[ICCG] also exhibits 2.3 times higher efficacy towards bPET powder with 36.5 % crystallinity. These observations suggest that LCC[ICCG] exhibits stronger PET-degrading activity than *Dm*PETase in these samples, but also reveal an underlying trend between the correlation of enzymes' PET activity. Specifically, the ratio of LCC[ICCG] to *Dm*PETase hydrolysis

products decreases with increasing crystallinity, indicating that LCC^{ICCG} PET-degrading activity is strongly impacted by crystallinity alteration, whereas DmPETase exhibits less sensitivity to this change. Indeed, this trend is confirmed as notably both PET-hydrolases have the same degrading efficiency towards the most crystalline PET sample (cPET-40 %).

Overall, our findings indicate that LCC^{ICCG} demonstrates significant degradation yields in low crystallinity PET, which is expected as the variant was engineered to specifically target the hydrolysis of amorphized post-consumer PET. However, the crystallinity degree of cPET (41%), considerably reduces LCC^{ICCG}'s degradation efficiency, likely by impeding enzyme approach to the material, as evidenced by a 10-fold lower product release compared to aPET. Conversely, although DmPETase shows a lower degradation yield on aPET, it seems to exhibit greater affinity for semi-crystalline PET materials with only a 4-fold lower yield. This difference can be attributed to the distinct electrostatic surface properties of the two enzymes. The combination of a lower degradation rate but better affinity to semi-crystalline PET balances LCC^{ICCG}'s activity on cPET. As a result, DmPETase was demonstrated to be equally effective in degrading semi-crystalline PET as LCC^{ICCG}.

4. Conclusions

In this study, the investigation of a novel promising PETase from the bacterium *D. maricopensis* (*Dm*PETase) was reported. While homologous to many characterized thermophilic PET-degrading enzymes, *Dm*PETase displays unique characteristics forming its own sub-branch on the phylogenetic tree and displaying dissimilar electrostatic surface to well-known benchmark PETases. *Dm*PETase characterization depicted a thermostable cutinase-like enzyme with the ability to degrade various synthetic polymers. Focusing on PET, *Dm*PETase was capable of degrading crystalline compartments of PET bottles, as well as semi-crystalline PET powder at the same level as LCC^{ICCG}, an industrially relevant enzyme, while getting less affected by PET crystallinity grade. These findings surpass previous reports and establish *Dm*PETase as a promising enzymatic platform for protein engineering, mainly around its active cite, enhancing PET degradation rate in combination with the enzyme's natural high affinity to semi-crystalline PET.

Funding

References

[1]   H. org/knowledge-hub/plastics-the-fact.-2022/ PlasticEurope: Plastics – The Facts 2022, Plastics – the Facts 2022, (2022).

[2]   P. Pandey, M. Dhiman, A. Kansal, S.P. Subudhi, Plastic waste management for sustainable environment: techniques and approaches, Waste Dispos. Sustain. Energy 2023. 5 (2023) 1–18. https://doi.org/10.1007/S42768-023-00134-6.

[3]   J.P. da Costa, P.S.M. Santos, A.C. Duarte, T. Rocha-Santos, (Nano)plastics in the environment - Sources, fates and effects, Sci. Total Environ. 566–567 (2016) 15–26. https://doi.org/10.1016/j.scitotenv.2016.05.041.

[4]   J. Siddiqui, G. Pandey, A Review of Plastic Waste Management Strategies, Int. Res. J. Environ. Sci. Int. Sci. Congr. Assoc. 2 (2013) 84–88. www.isca.me.

[5]   R. Geyer, J.R. Jambeck, K.L. Law, Production, use, and fate of all plastics ever made - Supplementary Information, Sci. Adv. 3 (2017) e1700782. https://doi.org/10.1126/sciadv.1700782.

[6]   I.E. Napper, B.F.R. Davies, H. Clifford, S. Elvin, H.J. Koldewey, P.A. Mayewski, K.R. Miner, M. Potocki, A.C. Elmore, A.P. Gajurel, R.C. Thompson, Reaching New Heights in Plastic Pollution—Preliminary Findings of Microplastics on Mount Everest, One Earth. 3 (2020) 621–630. https://doi.org/10.1016/j.oneear.2020.10.020.

[7]   S. Chiba, H. Saito, R. Fletcher, T. Yogi, M. Kayo, S. Miyagi, M. Ogido, K. Fujikura, Human footprint in the abyss: 30 year records of deep-sea plastic debris, Mar. Policy. 96 (2018) 204–212. https://doi.org/10.1016/j.marpol.2018.03.022.

[8]   P. Benyathiar, P. Kumar, G. Carpenter, J. Brace, D.K. Mishra, Polyethylene Terephthalate (PET) Bottle-to-Bottle Recycling for the Beverage Industry: A Review, Polymers (Basel). 14 (2022) 2366. https://doi.org/10.3390/polym14122366.

[9]   N. Mohanan, Z. Montazer, P.K. Sharma, D.B. Levin, Microbial and Enzymatic Degradation of Synthetic Plastics, Front. Microbiol. 11 (2020) 580709.

https://doi.org/10.3389/fmicb.2020.580709.

[10] N.E. Wallace, M.C. Adams, A.C. Chafin, D.D. Jones, C.L. Tsui, T.D. Gruber, The highly crystalline PET found in plastic water bottles does not support the growth of the PETase-producing bacterium Ideonella sakaiensis, Environ. Microbiol. Rep. 12 (2020) 578–582. https://doi.org/10.1111/1758-2229.12878.

[11] T. Sang, C.J. Wallis, G. Hill, G.J.P. Britovsek, Polyethylene terephthalate degradation under natural and accelerated weathering conditions, Eur. Polym. J. 136 (2020) 109873. https://doi.org/10.1016/j.eurpolymj.2020.109873.

[12] W. Wang, J. Ge, X. Yu, H. Li, Environmental fate and impacts of microplastics in soil ecosystems: Progress and perspective, Sci. Total Environ. 708 (2020) 134841. https://doi.org/10.1016/j.scitotenv.2019.134841.

[13] P.E. Redondo-Hasselerharm, G. Gort, E.T.H.M. Peeters, A.A. Koelmans, Nano- And microplastics affect the composition of freshwater benthic communities in the long term, Sci. Adv. 6 (2020) eaay4054. https://doi.org/10.1126/SCIADV.AAY4054/SUPPL_FILE/AAY4054_SM.PD F.

[14] K. Cverenkárová, M. Valachovičová, T. Mackul'ak, L. Žemlička, L. Bírošová, Microplastics in the Food Chain, Life. 11 (2021) 1349. https://doi.org/10.3390/LIFE11121349.

[15] N.A. Rorrer, S. Nicholson, A. Carpenter, M.J. Biddy, N.J. Grundl, G.T. Beckham, Combining Reclaimed PET with Bio-based Monomers Enables Plastics Upcycling, Joule. 3 (2019) 1006–1027. https://doi.org/10.1016/j.joule.2019.01.018.

[16] S. Kaabel, J.P. Daniel Therien, C.E. Deschênes, D. Duncan, T. Friščic, K. Auclair, Enzymatic depolymerization of highly crystalline polyethylene terephthalate enabled in moist-solid reaction mixtures, Proc. Natl. Acad. Sci. U. S. A. 118 (2021) e2026452118. https://doi.org/10.1073/pnas.2026452118.

[17] B.K.H. Lim, E.S. Thian, Biodegradation of polymers in managing plastic waste — A review, Sci. Total Environ. 813 (2022) 151880. https://doi.org/10.1016/j.scitotenv.2021.151880.

[18] A. Chamas, H. Moon, J. Zheng, Y. Qiu, T. Tabassum, J.H. Jang, M. Abu-Omar, S.L. Scott, S. Suh, Degradation Rates of Plastics in the Environment, ACS Sustain. Chem. Eng. 8 (2020) 3494–3511. https://doi.org/10.1021/acssuschemeng.9b06635.

[19] S.M. Emadian, T.T. Onay, B. Demirel, Biodegradation of bioplastics in natural environments, Waste Manag. 59 (2017) 526–536. https://doi.org/10.1016/j.wasman.2016.10.006.

[20] T. Narancic, K.E. O'Connor, Plastic waste as a global challenge: Are biodegradable plastics the answer to the plastic waste problem?, Microbiol. (United Kingdom). 165 (2019) 129–137. https://doi.org/10.1099/mic.0.000749.

[21] Y.H.V. Soong, M.J. Sobkowicz, D. Xie, Recent Advances in Biological Recycling of Polyethylene Terephthalate (PET) Plastic Wastes, Bioengineering. 9 (2022) 98. https://doi.org/10.3390/bioengineering9030098.

[22] E. Nikolaivits, B. Pantelic, M. Azeem, G. Taxeidis, R. Babu, E. Topakas, M. Brennan Fournet, J. Nikodinovic-Runic, Progressing Plastics Circularity: A Review of Mechano-Biocatalytic Approaches for Waste Plastic (Re)valorization, Front. Bioeng. Biotechnol. 9 (2021) 696040. https://doi.org/10.3389/fbioe.2021.696040.

[23] V. Tournier, S. Duquesne, F. Guillamot, H. Cramail, D. Taton, A. Marty, I. André, Enzymes' Power for Plastics Degradation, Chem. Rev. (2023). https://doi.org/10.1021/acs.chemrev.2c00644.

[24] S. Sulaiman, S. Yamato, E. Kanaya, J.J. Kim, Y. Koga, K. Takano, S. Kanaya, Isolation of a novel cutinase homolog with polyethylene terephthalate-degrading activity from leaf-branch compost by using a metagenomic approach, Appl. Environ. Microbiol. 78 (2012) 1556–1562. https://doi.org/10.1128/AEM.06725-11.

[25] V. Tournier, C.M. Topham, A. Gilles, B. David, C. Folgoas, E. Moya-Leclair, E. Kamionka, M.L. Desrousseaux, H. Texier, S. Gavalda, M. Cot, E. Guémard, M. Dalibey, J. Nomme, G. Cioci, S. Barbe, M. Chateau, I. André, S. Duquesne, A. Marty, An engineered PET depolymerase to break down and recycle plastic

bottles, Nature. 580 (2020) 216–219. https://doi.org/10.1038/s41586-020-2149-4.

[26] Z. Ding, G. Xu, R. Miao, N. Wu, W. Zhang, B. Yao, F. Guan, H. Huang, J. Tian, Rational redesign of thermophilic PET hydrolase LCCICCG to enhance hydrolysis of high crystallinity polyethylene terephthalates, J. Hazard. Mater. 453 (2023) 131386. https://doi.org/10.1016/J.JHAZMAT.2023.131386.

[27] S. Thiyagarajan, E. Maaskant-Reilink, T.A. Ewing, M.K. Julsing, J. Van Haveren, Back-to-monomer recycling of polycondensation polymers: Opportunities for chemicals and enzymes, RSC Adv. 12 (2022) 947–970. https://doi.org/10.1039/d1ra08217e.

[28] S. Gibson, S. Walter, G.M. Gübitz, Enzymes for the Biofunctionalization of PET, in: Biofunctionalization Polym. Their Appl., Springer, Berlin, Heidelberg, 2011: p. 107. https://doi.org/10.1007/10_2010_91.

[29] R.J. Young, P.A. Lovell, The glass transition, in: Introd. to Polym., 3rd ed., Taylor & Francis Group, 2011: p. 384.

[30] J.M. Hutchinson, Physical aging of polymers, Prog. Mater. Sci. 20 (1995) 703–760. https://doi.org/https://doi.org/10.1016/0079-6700(94)00001-I.

[31] R. Wei, D. Breite, C. Song, D. Gräsing, T. Ploss, P. Hille, R. Schwerdtfeger, J. Matysik, A. Schulze, W. Zimmermann, Biocatalytic Degradation Efficiency of Postconsumer Polyethylene Terephthalate Packaging Determined by Their Polymer Microstructures, Adv. Sci. 6 (2019) 1900491. https://doi.org/10.1002/advs.201900491.

[32] S. Yoshida, K. Hiraga, T. Takehana, I. Taniguchi, H. Yamaji, Y. Maeda, K. Toyohara, K. Miyamoto, Y. Kimura, K. Oda, A bacterium that degrades and assimilates poly(ethylene terephthalate), Science (80-.). 351 (2016) 1196–1199. https://doi.org/10.1126/science.aad6359.

[33] H. Lu, D.J. Diaz, N.J. Czarnecki, C. Zhu, W. Kim, R. Shroff, D.J. Acosta, B.R. Alexander, H.O. Cole, Y. Zhang, N.A. Lynd, A.D. Ellington, H.S. Alper, Machine learning-aided engineering of hydrolases for PET depolymerization, Nature. 604 (2022) 662–667. https://doi.org/10.1038/s41586-022-04599-z.

[34] F. Teufel, J.J. Almagro Armenteros, A.R. Johansen, M.H. Gíslason, S.I. Pihl, K.D. Tsirigos, O. Winther, S. Brunak, G. von Heijne, H. Nielsen, SignalP 6.0 predicts all five types of signal peptides using protein language models, Nat. Biotechnol. 40 (2022) 1023–1025. https://doi.org/10.1038/s41587-021-01156-3.

[35] E. Nikolaivits, A. Kokkinou, M. Karpusas, E. Topakas, Microbial host selection and periplasmic folding in Escherichia coli affect the biochemical characteristics of a cutinase from Fusarium oxysporum, Protein Expr. Purif. 127 (2016) 1–7. https://doi.org/10.1016/j.pep.2016.06.002.

[36] E. Gasteiger, C. Hoogland, A. Gattiker, S. Duvaud, M.R. Wilkins, R.D. Appel, A. Bairoch, Protein Identification and Analysis Tools on ExPASy Server, in: J.M. Walker (Ed.), Proteomics Protoc. Handb., 1st ed., Humana Totowa, NJ, 2005: pp. 571–607. https://doi.org/10.1385/1592598900.

[37] E. Nikolaivits, G. Taxeidis, C. Gkountela, S. Vouyiouka, V. Maslak, J. Nikodinovic-Runic, E. Topakas, A polyesterase from the Antarctic bacterium Moraxella sp. degrades highly crystalline synthetic polymers, J. Hazard. Mater. 434 (2022) 128900. https://doi.org/10.1016/j.jhazmat.2022.128900.

[38] D. Danso, C. Schmeisser, J. Chow, New Insights into the Function and Global Distribution of Polyethylene Terephthalate (PET) -Degrading Bacteria and, Appl. Environ. Microbiol. 84 (2018) e02773-17. https://doi.org/10.1128/AEM.02773-17.

[39] W. Zeng, X. Li, Y. Yang, J. Min, J.W. Huang, W. Liu, D. Niu, X. Yang, X. Han, L. Zhang, L. Dai, C.C. Chen, R.T. Guo, Substrate-Binding Mode of a Thermophilic PET Hydrolase and Engineering the Enzyme to Enhance the Hydrolytic Efficacy, ACS Catal. 12 (2022) 3033–3040. https://doi.org/10.1021/acscatal.1c05800.

[40] B. Zhu, D. Wang, N. Wei, Enzyme discovery and engineering for sustainable plastic recycling, Trends Biotechnol. 40 (2022) 22–37. https://doi.org/10.1016/j.tibtech.2021.02.008.

[41] H.Y. Sagong, H.F. Son, H. Seo, H. Hong, D. Lee, K.J. Kim, Implications for the PET decomposition mechanism through similarity and dissimilarity between

PETases from Rhizobacter gummiphilus and Ideonella sakaiensis, J. Hazard. Mater. 416 (2021) 126075. https://doi.org/10.1016/j.jhazmat.2021.126075.

[42] E. Herrero Acero, D. Ribitsch, A. Dellacher, S. Zitzenbacher, A. Marold, G. Steinkellner, K. Gruber, H. Schwab, G.M. Guebitz, Surface engineering of a cutinase from Thermobifida Cellulosilytica for improved polyester hydrolysis, Biotechnol. Bioeng. 110 (2013) 2581–2590. https://doi.org/10.1002/bit.24930.

[43] T. Miyakawa, H. Mizushima, J. Ohtsuka, M. Oda, F. Kawai, M. Tanokura, Structural basis for the Ca2+-enhanced thermostability and activity of PET-degrading cutinase-like enzyme from Saccharomonospora viridis AHK190, Appl. Microbiol. Biotechnol. 99 (2015) 4297–4307. https://doi.org/10.1007/s00253-014-6272-8.

[44] C.M. Carr, D.J. Clarke, A.D.W. Dobson, Microbial Polyethylene Terephthalate Hydrolases : Current and Future Perspectives, Front. Microbiol. 11 (2020) 571265. https://doi.org/10.3389/fmicb.2020.571265.

[45] E. Nikolaivits, M. Kanelli, M. Dimarogona, E. Topakas, A middle-aged enzyme still in its prime: Recent advances in the field of cutinases, Catalysts. 8 (2018) 612. https://doi.org/10.3390/catal8120612.

[46] N. Flores-Castañón, S. Sarkar, A. Banerjee, Structural, functional, and molecular docking analyses of microbial cutinase enzymes against polyurethane monomers, J. Hazard. Mater. Lett. 3 (2022) 100063. https://doi.org/10.1016/j.hazl.2022.100063.

[47] A. Kemona, M. Piotrowska, Polyurethane recycling and disposal: Methods and prospects, Polymers (Basel). 12 (2020) 1752. https://doi.org/10.3390/POLYM12081752.

[48] S. Giraldo-Narcizo, N. Guenani, A.M. Sánchez-Pérez, A. Guerrero, Accelerated Polyethylene Terephthalate (PET) Enzymatic Degradation by Room Temperature Alkali Pre-treatment for Reduced Polymer Crystallinity, ChemBioChem. 24 (2023) e202200503. https://doi.org/10.1002/cbic.202200503.

[49] A.A. Natu, E.A. Lofgren, S.A. Jabarin, Effect of morphology on barrier

properties of poly(ethylene terephthalate), Polym. Eng. Sci. 45 (2005) 400–409. https://doi.org/10.1002/pen.20288.

[50] T.L. Phillips, R. Harris, A.R. Burgess, J. Johnston, Colored polyethylene terephthalate composition and process of its manufacture, 5,686,515, 1997.

Table 1 Michaelis-Menten kinetic parameters for the hydrolysis of pNPA, pNPB, pNPO and pNPD catalyzed by DmPETase and LCC^{ICCG}.

Substrate	K_M (mM)		k_{cat} (s^{-1})		k_{cat}/K_M (s$^{-1}\times$mM^{-1})		DmPETase /LCC^{ICCG}
	DmPETase	LCC^{ICCG}	DmPETase	LCC^{ICCG}	DmPETase	LCC^{ICCG}	
pNPA	0.90 ± 0.04	7.31 ± 1.04	27.54 ± 0.69	159.17 ± 15.84	30.58 ± 1.46	21.75 ± 5.27	1.41 ± 0.41
pNPB	0.19 ± 0.02	0.76 ± 0.10	30.78 ± 1.41	136.72 ± 5.66	158.80 ± 18.89	180.11 ± 31.51	0.88 ± 0.26
pNPO	1.29 ± 0.23	7.44 ± 2.46	11.33 ± 1.54	106.54 ± 21.82	8.82 ± 1.21	14.32 ± 5.15	0.62 ± 0.21
pNPD	0.93 ± 0.09	2.68 ± 0.46	2.47 ± 0.15	8.11 ± 0.78	2.68 ± 0.30	3.02 ± 0.81	0.89 ± 0.34

Table 2 Concentration of water-soluble products released after enzymatic treatment of different PET powders of various crystallinities with *Dm*PETase and LCC^{ICCG}. Reactions took place at 50 °C for 72 h. Control reactions were performed in the absence of enzyme under the same conditions.

Enzyme	Concentration of water-soluble hydrolysis products ($\mu g_{PRODUCT}/mg_{PET}$)				
	aPET (x_c 6 %)	tPET (x_c 21 %)	gPET (x_c 21 %)	cPET (x_c 40 %)	bPET (x_c 36 %)
*Dm*PETase	119.45 ± 10.13	54.27 ± 6.89	35.77 ± 2.67	30.30 ± 1.66	7.81 ± 0.29
LCC^{ICCG}	413.71 ± 8.76	164.13 ± 9.81	96.73 ± 4.52	35.02 ± 2.49	18.33 ± 1.68
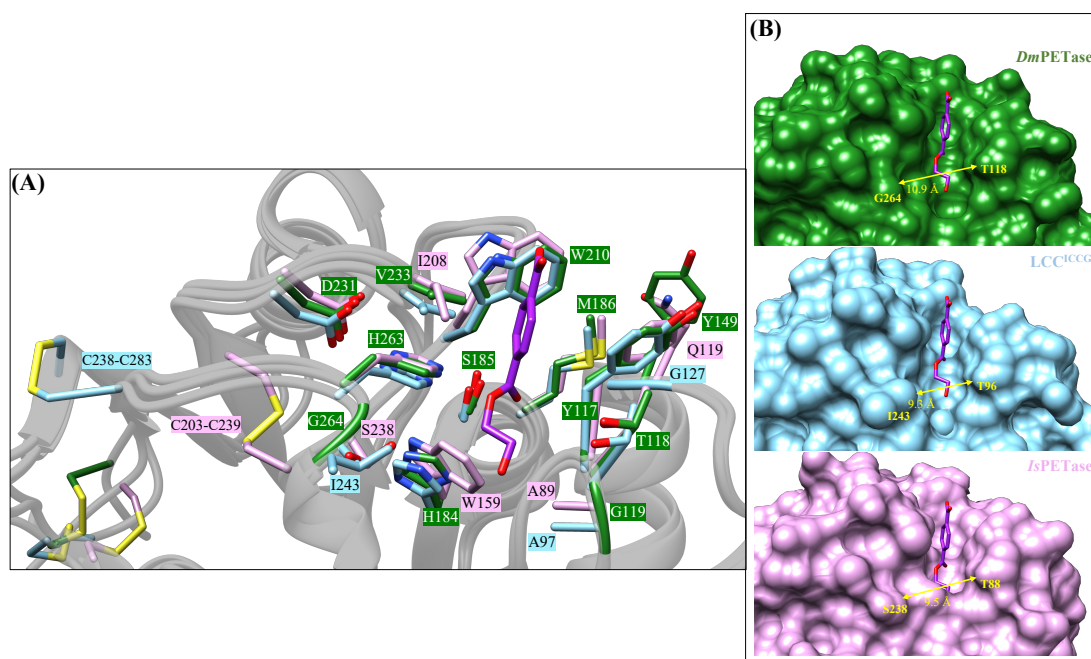
Figure 1 (A) Superimposition of *Dm*PETase (green) with LCC[ICCG] (blue-PDB ID 7VVE) and *Is*PETase (pink- PDB ID 6EQH), highlighting important residues participating in structural features (cysteines for disulfide bonds) or catalytic and substrate binding. Ligand 2-hydroxyethyl terephthalate (MHET-magenta) as part of LCC[ICCG] is also presented. (B) Surface representation of the three enzymes focusing on the substrate-binding site as indicated by the position of MHET (magenta). Distances indicating the width of the binding site.
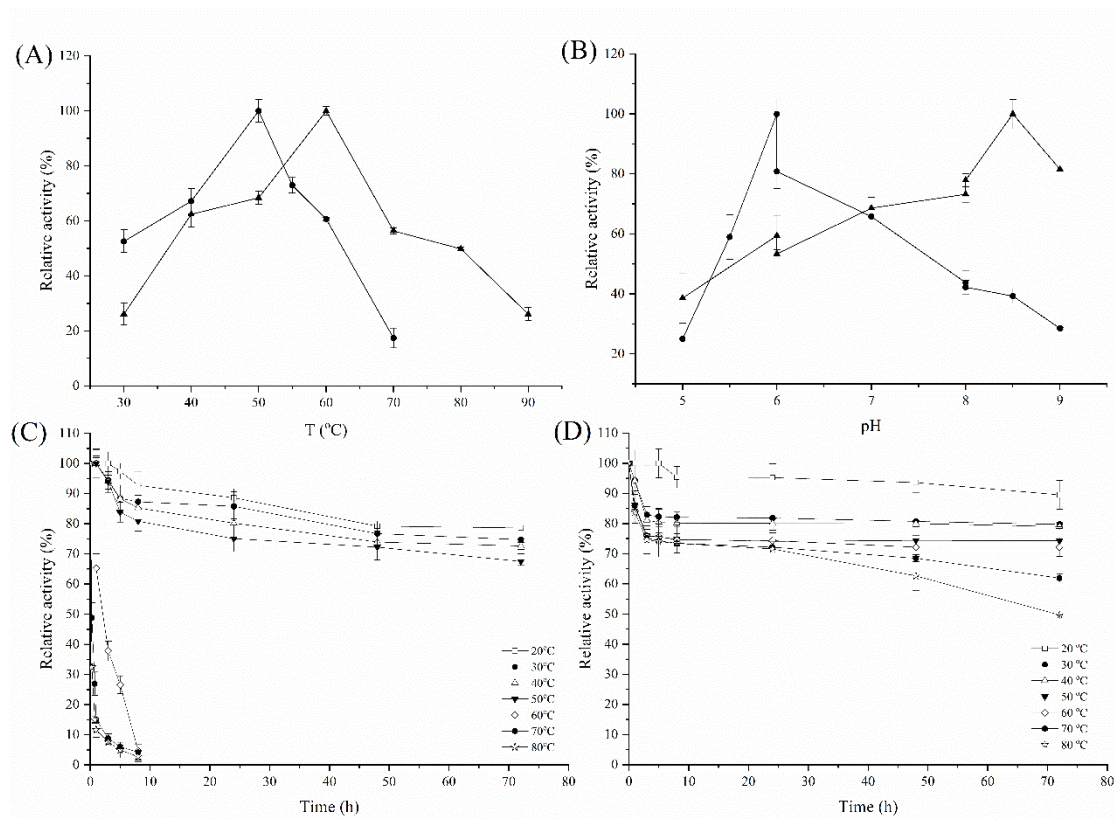
Figure 2 (A) Effect of temperature on the activity of *Dm*PETase (●) and LCC[ICCG]
(▲). Relative activity was defined after assaying *Dm*PETase and LCC[ICCG] with pNPB
in phosphate-citrate buffer (pH 6.0). **(B)** Effect of pH on the activity of *Dm*PETase
(●) and LCC[ICCG] (▲). Relative activity was defined after assaying with pNPB in a
variety of buffer systems, at 35 °C. Buffer systems used were citrate-phosphate (pH
5.0-6.0), sodium-phosphate (pH 6.0-8.0) and Tris-HCl (pH 8.0-9.0). Effect of
temperature on the stability of *Dm*PETase **(C)** and LCC[ICCG] **(D)**. Relative activity was
defined after incubating the enzymes in 25 mM Tris-HCl pH 7.4, 150 mM NaCl
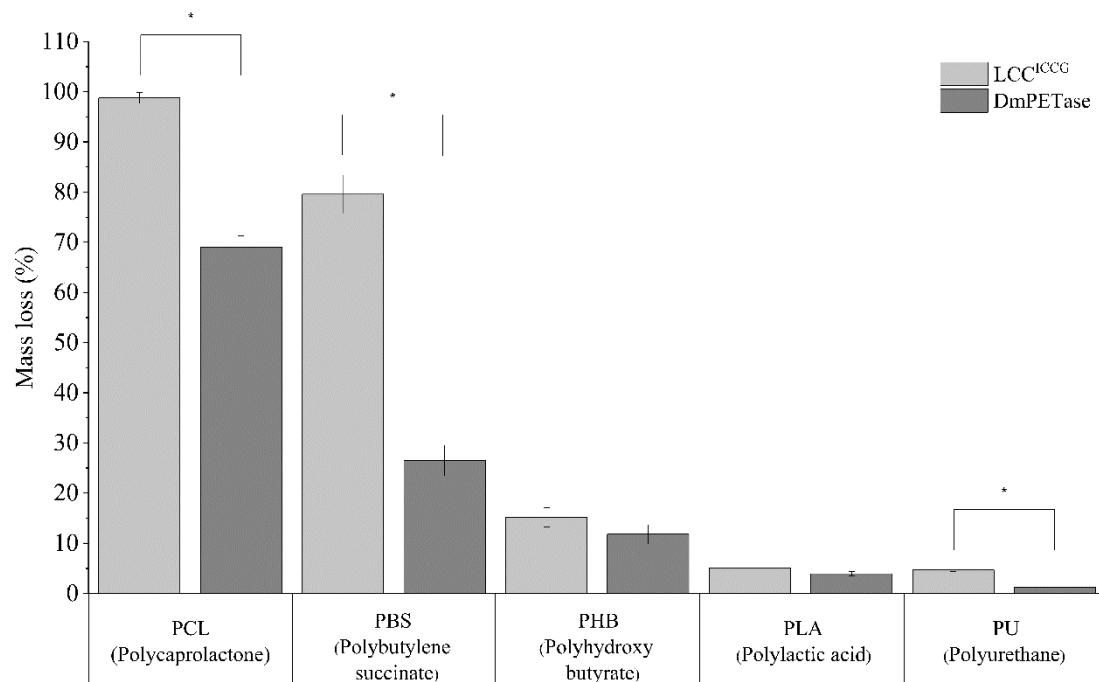buffer at temperatures ranging from 20-80 °C for up to 72 h.

Figure 3 Dry mass loss (%) of different synthetic polymers after their treatment with *Dm*PETase (dark grey) and LCC[ICCG] (light grey). Reactions took place at 50 °C for 72 h (except from PCL, for 24 h). Control reactions in the absence of enzyme were performed under the same conditions and dry mass loss, whenever existed, was subtracted from the enzymatic reactions' results. Asterisk brackets represent statistically significant differences between corresponding values, according to Independent-Samples t-Test with a significance level of p-value < 0.05.
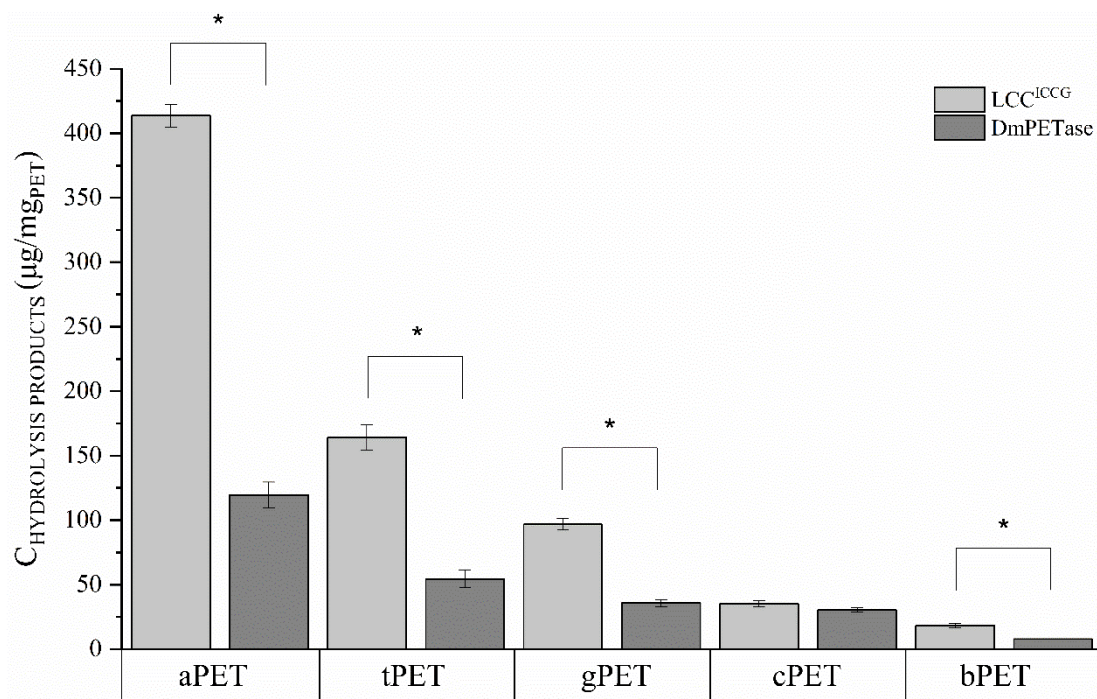
Figure 4 Water-soluble products released after treating different powdered PET materials of variable crystallinities with DmPETase and LCC^{ICCG}. Materials: aPET-amorphous PET of x_c 5 %, tPET-transparent PET bottle of x_c 21 %, gPET-green PET bottle of x_c 21 %, cPET-semi-crystalline PET of x_c 41 % and bPET-POLIPET of x_c 36 %. Reactions took place at 50 °C for 72 h. Control reactions in the absence of enzyme were performed under the same conditions and dry mass loss, whenever existed, was subtracted from the enzymatic reactions' results. Asterisk brackets represent statistically significant differences between corresponding values, according to Independent-Samples t-Test with a significance level of p-value < 0.05.
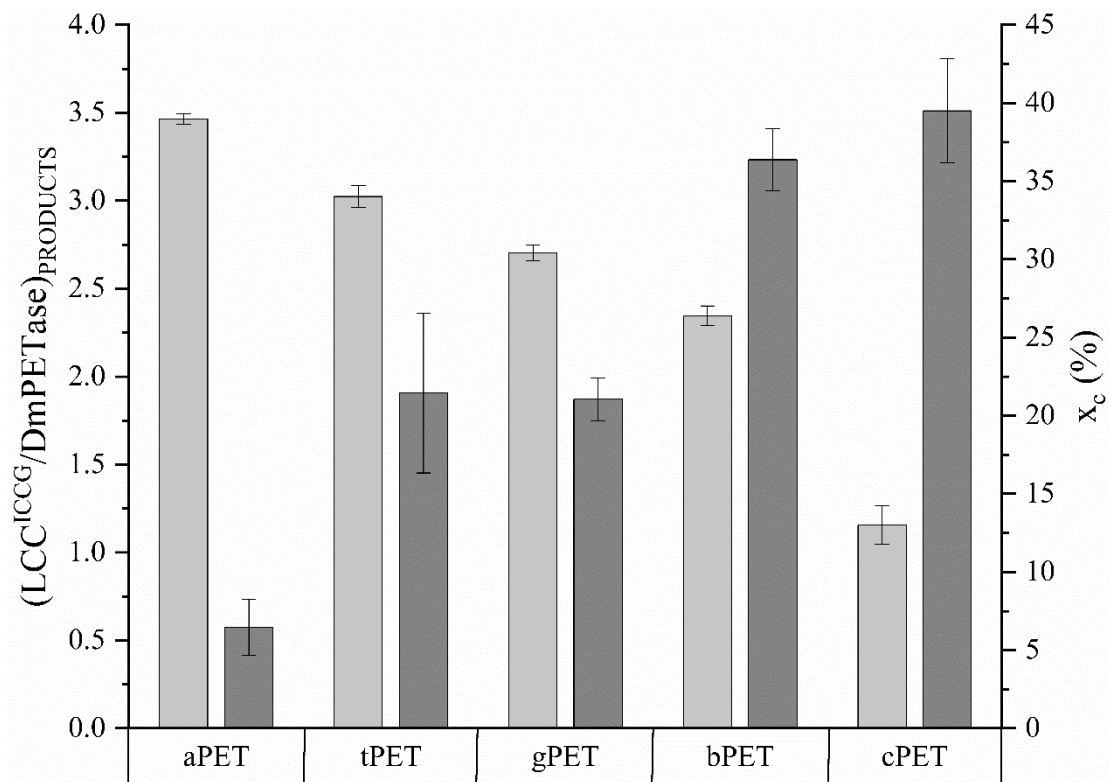
Figure 5 Ratio of hydrolysis products released by LCC^{ICCG} to *Dm*PETase (light grey) of PET powders of variable crystallinities (dark grey).